

Mini Review

Current Trends in Electrochemical Aptasensor for Tumor-Associated Growth Factor Receptor Detection in Serum

Li Han^{1,2}

¹ Zhang Zhongjing College of Chinese Medicine, Nanyang Institute of Technology, Nanyang, 473004, China

² Henan Key Laboratory of Zhang Zhongjing Formulae and Herbs for Immunoregulation, Nanyang Institute of Technology, Nanyang, 473004, China

E-mail: luckyhanllyistt666@163.com

Received: 9 March 2022 / Accepted: 16 April 2022 / Published: 7 May 2022

Cancer is a kind of malignant disease that seriously endangers human health. The change of growth factor content in serum is considered to be of great significance for the diagnosis and prognosis of cancer. Therefore, developing a low-cost rapid detection of various growth factors in serum is necessary. This review focuses on fabricating an electrochemical aptasensor for the sensing of growth factors in serum. Especially, epidermal growth factor receptor, vascular endothelial growth factor, and platelet-derived growth factor were described in detail. In addition, the future development direction of electrochemical adaptor sensors has been prospected in this review, which will provide a reference for further research and application.

Keywords: Aptasensor; Vascular endothelial growth factor; Epidermal growth factor receptor; Platelet-derived growth factor; Electroanalysis

1. INTRODUCTION

Cancer has become one of the world's highest mortality rates, with the World Health Organization predicting that 12 million people will die of cancer globally by 2030. More than 200 cancers have been found, and they can have a severe impact on more than 60 organs. Clinical studies have found that the five-year relative survival rate of patients with advanced cancer is much lower than those diagnosed at an early stage [1,2]. Cancer markers can be used as the basis for cancer screening and disease monitoring, so the sensitivity sensing of cancer markers is crucial for the early diagnosis [3–5]. The electrochemical aptasensor has the advantages of high sensitivity, reasonable specificity, and rapid response. In the fabrication of the sensor, an efficient signal amplification strategy could enhance the performance, which is of great significance for the sensitive sensing of cancer markers [6–8].

Biomarkers are intracellular or intercellular molecules with important biological functions whose expression or activity can cause changes in the corresponding pathological conditions. The measurement and evaluation of biomarkers can be used as indicators of normal biological or pathogenic processes [9–11]. Each biomarker indicates a specific disease process, while cancer markers are used in oncology to aid in cancer study. Cancer markers are substances released by tumor cells or stimulated by tumors, including enzymes, nucleic acids, proteins, cells, etc. The information on cancer cell differentiation and tumor tissue genesis can be obtained through qualitative and quantitative sensing of cancer markers. This information provides the basis for cancer screening, disease monitoring, and cancer treatment [12,13]. Since only a tiny amount of cancer markers exist in the early stage of cancer, it is essential to develop a sensitive and accurate method to detect cancer markers in the early clinical diagnosis of cancer [14,15].

Aptamers were first reported in the 1990s. It is a functional nucleic acid screened from random sequences of DNA or RNA by the exponential enrichment technique (SELEX). It usually consists of 20–100 nucleotides and has a specific binding ability with the target [16–18]. Aptamers can form various secondary structures (hairpins, G-tetrahedron, rings, etc.). When the target molecule is present, the secondary structure can form a specific tertiary structure, which can be recognized with the target molecule [19–21]. This process is similar to the antigen-antibody binding process, so aptamers are also known as antibodies. Researchers have currently screened a variety of aptamers targeting small molecules, proteins, cells, tissues, viruses, etc. Compared with antibodies, aptamers have many advantages: easy synthesis, high selectivity, low cost, easy chemical modification, and good stability, so they are widely used in the construction of biosensor platforms [22–24].

The electrochemical biosensor consists of a molecular recognition element, signal conversion element, and electronic instrument [25–35]. Recognition elements are generally divided into receptors, enzymes, antibodies, nucleic acids, tissues, and cells. Electrochemical biosensors using aptamers as molecular recognition elements are called electrochemical aptasensor. The electrochemical aptasensor has the advantages of simplicity, reliability, low cost, and sensitivity. It can immobilize the aptamer on the electrode surface and detect and record the signal changes caused by biometric recognition of the electrochemical sensor after the aptamer is recognized explicitly with the target. In recent years, cutting-edge science such as medicine and nanoscience and electrochemical aptasensor technology, electrochemical aptasensor can detect a low content specific target in blood, urine, or saliva, providing a sensitive direct measurement method for the detection of cancer markers [36–40]. The electrochemical aptasensor used to detect cancer biomarkers can be divided into current, impedance, potential, and capacitance types according to the different detection signals. In this review, electrochemical aptasensor for detecting growth factor markers associated with cancer were summarized.

2. DETECTION OF EPIDERMAL GROWTH FACTOR RECEPTORS

Lung cancer is the most common malignant tumor with the highest incidence and death toll. Lung cancer can be divided into small cell lung cancer and non-small cell lung cancer, among which non-small cell lung cancer (NSCLC) accounted for 80% ~ 85% [41,42]. The development of molecular biomedicine and technology has promoted the in-depth understanding of the molecular level of NSCLC

and identified some important carcinogenic sites and biomolecules [43]. Among the significant biomolecules of NSCLC, the epidermal growth factor receptor (EGFR) is one of the most widely and deeply studied molecules. EGFR is present in almost all body tissues except the hematopoietic system. EGFR binds to ligands and cascades through specific signaling pathways, affecting cell proliferation, survival, differentiation, motility, and adhesion [44–46]. Studies have shown that abnormal expression, mutation, and abnormal expression of EGFR ligand can promote differentiation, proliferation, adhesion, invasion, and metastasis of tumor cells. It can also promote tumor angiogenesis and inhibit cell apoptosis [47].

Guo et al. [48] employed a two-dimensional CuNi organic framework as a linker to create a sensitive scaffold for electrochemical detection of adsorbed aptamer chains in C6 glioma cells and associated biomarker EGFR. In contrast to normal MOFs, this one has long-range delocalized electrons, graphene-like nanostructures, numerous metallic states, and abundant oxygen vacancies. Coordination between metal centers, oligonucleotides, stacking, and van der Waals forces may be used to immobilize many C6 cell-targeting aptamer chains. When the EGFR concentration was between 1 fg/mL and 1 ng/mL, the sensor demonstrated excellent selectivity, stability, and repeatability, with a LOD of 0.72 fg/mL. Bezerra et al. [49] created an aptasensor for EGFR2 sensing in human serum. They immobilized EGFR2 aptamers on the surface of handmade polylysine-modified SPE by electrostatic adsorption. As a redox indicator, methylene blue was employed. EGFR2 had a linear detection range of 10–60 ng/mL and a LOD of 3.0 ng/mL. In the absence of additional protein, a peak of 6.72 A was seen in the blood of a healthy lady. Additionally, they analyzed the serum of a breast cancer patient and received a 2.65 A signal. The same pattern was found when protein was introduced to the serum control group; the more clear the protein content, the weaker the signal. They used SEM and ITC to characterize the aptamer and discovered a firm contact between the aptamer and the target protein. Yan et al. [50] synthesized a p-COF using a simple oil tank process and employed it as a new sensing layer for immobilizing EGFR-targeting aptamer chains, allowing for the first time the detection of tiny levels of EGFR. p-COF possesses a nanosheet-like structure, large pores, an abundance of nitrogen-containing groups, intense electrochemical activity, high bioaffinity, low toxicity, and excellent solubility in water. Due to the creation of the aptamer-EGFR complex, the interaction between the aptamer chain and EGFR dramatically altered the electrochemical signal of the modified electrode. The LOD of the aptasensor based on p-COF is 5.64 fg/mL. The produced aptamer sensor exhibits a high degree of selectivity, stability, repeatability, and recyclability and is well suited for use with human serum samples. Wang et al. [51] synthesized an electrochemical paper-based aptamer for EGFR determination. The device utilizes the origami idea as a valve between sample input and detection, lowering sampling volume and increasing operator convenience (Figure 1). They changed the working electrode using amino-functionalized graphene/thionine/gold particle nanocomposites, which created electrochemical signals and provided an environment conducive to aptamer loading. Serum samples were analyzed to confirm the analytical reliability of the sensor suggested in this research, and the findings were consistent with those obtained using the gold standard ELISA.

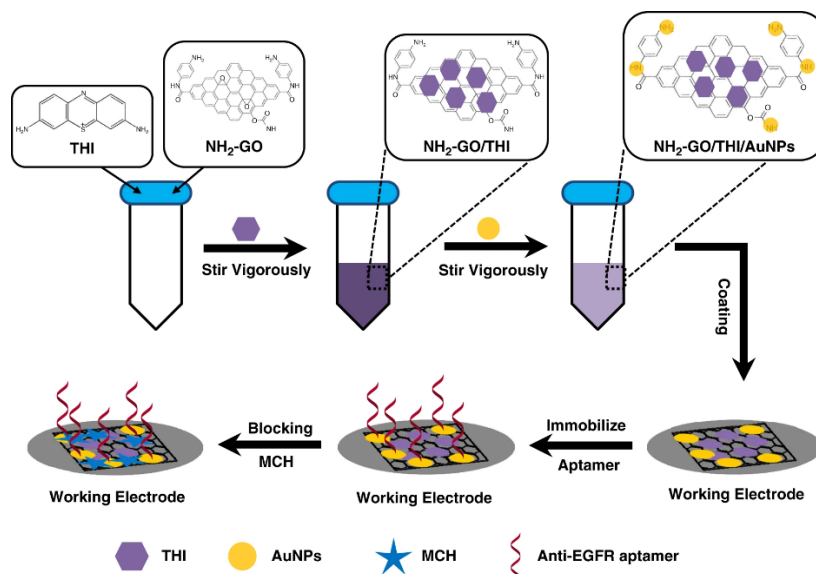


Figure 1. Scheme of fabrication of the origami-paper-based EGFR aptasensor (Copyright: Springer Nature) [51].

3. DETECTION OF VASCULAR ENDOTHELIAL GROWTH FACTOR

Angiogenesis is dependent on existing blood vessels and is an essential process involved in tumor growth. Since the critical role of angiogenic factors in tumor growth has been confirmed, a large number of studies focus on the regulatory mechanism of angiogenesis [52–54]. During the tumorigenesis stage, the "switch" of angiogenesis is related to initiating tumor cell expression and secretion. The degree of tumor angiogenesis depends on the antagonism between angiogenic and antiangiogenic factors [55–57]. Vascular Endothelial growth factor (VEGF) is one of the most effective angiogenic factors and has a specific division ability on endothelial cells. VEGF can induce endothelial cell proliferation, improve vascular permeability and promote protein extravasation [58]. This can lead to the growth of a fibrin matrix, making it possible for stromal cells to infiltrate into the formed tumor [59,60]. VEGF-mediated angiogenesis under hypoxia may be the primary mechanism involved in the growth of many tumors. Inhibiting VEGF expression *in vivo* has been shown to inhibit tumor growth [61–63].

Some scholars have recently observed the role of VEGF in differentiating benign and malignant tumors in circulation. For example, the level of VEGF in ovarian cancer is significantly higher than that in benign ovarian lesions, indicating the serum VEGF may have a diagnostic value [64]. Another practical clinical application is to monitor the recurrence of primary tumors after treatment, especially after surgery. Serum VEGF levels have decreased significantly after breast, colorectal and ovarian cancer [65–68]. Serum VEGF levels were observed to increase continuously or again after an initial decrease in patients with recurrent tumors after resectioning the primary tumor. In contrast, patients who did not relapse after surgical resection tended to have a sustained decrease in serum VEGF levels.

Zhao et al. [69] described a foldable electrochemical DNA-based sensor that directly determines VEGF in the biological matrix such as serum and whole blood. Electrochemical signal production is combined with methylene blue modification and substantial conformational changes in anti-VEGF aptamers loaded on the surface. The sensor can detect VEGF at concentrations as low as 5 pM.

Additionally, the sensor operates admirably when manufactured on gold-coated screen-printed carbon electrodes, indicating that it has the potential to be a low-cost, disposable biosensor for disease detection and treatment monitoring. Ravalli et al. [70] discussed the invention of a single-use electrochemical aptasensor for VEGF detection. The gold nanostructured graphite electrodes were initially modified using a mixed monolayer of thiolated DNA aptamers and 6-mercapto-1-hexanol as a spacer thiol. Following that, the VEGF protein was incubated with an aptasensor. The methodology for detecting enzymatic amplification employs a streptavidin-alkaline phosphatase conjugate with a biotinylated secondary aptamer. This enzyme catalyzes the hydrolysis of electroactive 1-naphthalene phosphate to 1-naphthol. The resulting product was electroactive and was identified using DPV. The aptasensor responded linearly to the target concentration between 0 and 250 nM; the LOD was 30 nM. Ni et al. [71] created an electrochemical aptasensor based on a molecular beacon for the ratiometric measurement of VEGF in serum. The surface of the nanocomposites was modified using graphene oxide/methylene blue and AuNPs, followed by the addition of ferrocene-labeled aptamers to VEGF (aptamer-Fc). The presence of VEGF may cause a conformational shift in the aptamer-Fc, leading the redox probe Fc to migrate away, weakening the electrochemical connection between the electrode and the Fc. Simultaneously, the methylene blue signal decreased due to the aptamer-FC obstructing the electron transport channel. The developed sensing interface may be utilized to detect VEGF in real-time using a ratiometric dual signal readout with a 2-500 pg/mL linear detection range. The LOD can achieve to be 0.1 pg/mL. Another study quantified VEGF in serum using dual electrochemical signal mode ratio measurement by altering graphene oxide loaded with methylene blue and a ferrocene-labeled aptamer on GCE [72]. To compare, scientists created two sensing surfaces composed of graphene oxide and methylene blue covalently bonded and physically adsorbed. Structural switch aptamers tagged with the redox compound ferrocene bind to VEGF and operate as recognition probes, providing an electrochemical signal readout in the presence of the analyte. Sensors that are covalently bonded have a more significant number of aptamers than physically adsorbed sensors but have relative stability. The linear detection ranges for VEGF were 10-500 pg/mL and 20-500 pg/mL, respectively. In comparison to single-signal mode detection, this strategy's sensor surface allows VEGF measurement in dual-signal mode with a greater linear range.

Lv et al. [73] developed a biosensor for VEGF concentration measurement using a novel technique for fabricating an elegant electrochemical aptasensor. One electroactive probe, heme, was not covalently changed at the oligonucleotide's end in our technique. This approach is straightforward, inexpensive, and capable of monitoring VEGF at concentrations as low as 1 nM. Fu et al. [74] effectively synthesized DNA-templated Ag/Pt bimetallic nanoclusters using an improved synthesis process. These nanocomposites have peroxidase-like activity and can catalyze the substrate's oxidation of 3,3',5,5'-tetramethylbenzidine by H_2O_2 to produce a blue product. They developed a label-free electrochemical aptasensor for VEGF sensing based on this characteristic utilizing VEGF's aptamer. The linear relationship was excellent between 6.0 and 20 pM under optimum experimental conditions, and the LOD was 4.6 pM. The aptasensor is highly specific for VEGF and can directly detect the level of VEGF in breast cancer patients' serum. Nonaka et al. [75] devised a technique for detecting VEGF that utilizes two VEGF-binding aptamers. In this investigation, VEGF-A was detected utilizing a sandwich technique that included a VEGF-binding aptamer tagged with pyridinequinoline quinone glucose dehydrogenase

and another aptamer mounted on a gold wire electrode superior. For this approach, we investigated several combinations of VEGF-binding aptamers. Additionally, we investigated the dosage dependency of the current generated by pyridinequinoline quinone glucose dehydrogenase in the VEGF detection system that we created. They effectively-identified VEGF165 at a concentration of 15 nM. Wang et al. [76] created a unique gold nanostructure embedded in chitosan (Au-C) and employed it as a platform for detecting VEGF165. Compared to the hollow pristine Au, the chitosan in Au covers the full surface of the framework and fills the interior, and the structure is reasonably robust, enhancing the electrical conductivity and electrochemical activity of Au-C. The Au-C combination was employed as the sensitive layer, and the VEGF165-antiaptamer chain was used to produce an electrochemical aptasensor. Because the Au-C composites combine the benefits of chitosan biocompatibility, Au bioaffinity, and the hollow framework, the developed aptasensor has a high sensitivity to VEGF165 with a LOD of 6.77 pg/mL. Tabrizi et al. [77] fabricated a label-free electrochemical conformal sensor for the sensing of VEGF165. They used CV and EIS to investigate the electrochemical behavior of the biosensors they had manufactured. The aptasensor operates on the idea that when the anti-VEGF165 aptamer immobilized on the electrode surface interacts with the VEGF165 tumor marker in the sample solution, the electrode interface characteristics change. This alters the interfacial charge transfer resistance, which EIS may measure. The aptasensor demonstrated an excellent linear relationship in 10.0 to 300.0 pg/mL. The developed aptasensor was effectively used to detect VEGF165 in serum samples from patients with lung cancer. Park et al. [78] fabricated a label-free electrochemical aptasensor sensor using carbon nanotubes and polyaniline nanocomposites to detect the tumor marker VEGF165. The nanocomposite was built into a susceptible VEGF165 sensor using an immobilized VEGF165 aptamer (Figure 2). Due to the complementing action of PANI/CNT, the linear range is broad and steady between 0.5 pg/mL and 1 g/mL, and the LOD is 0.4 pg/mL.

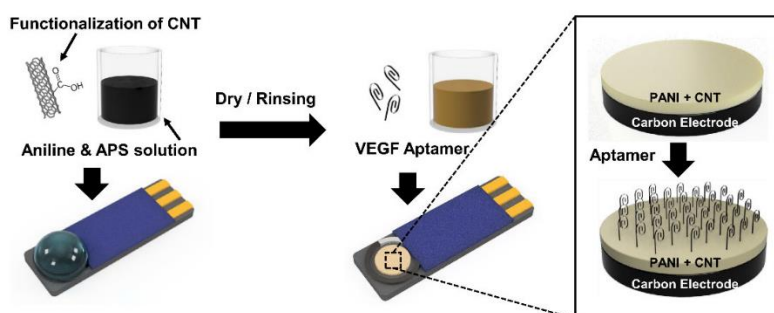


Figure 2. Scheme of the VEGF165 electrochemical aptasensor fabrication. (Copyright: MDPI) [78].

Gao et al. [79] describe a biosensor incorporating scaffold-mediated strand displacement cyclic amplification and a VEGF aptamer. Hybridization of probe A with the VEGF aptamer lead to the formation of a probe A-aptamer complex. When VEGF is added, the aptamer attaches specifically to it, allowing probe A to be released. Then, free probe A catches Hp1's plantar site, exposing the plantar site at the other end of Hp1. Similarly, Hp2 and Hp3 were immobilized on the electrode surface. Thus,

methylene blue induced a current response on Hp2 and Hp3. The amount of VEGF expression may be quantified using the signal transduction process. Cheng et al. [80] also created an electrochemical aptasensor. When the mounted aptamer-hairpin probe comes into contact with the protein target, it detects the protein, initiates a primer extension process through the target-induced conformational change, and releases the protein from the duplicated DNA duplex. The released target molecule may cyclically interact with additional aptamer-hairpin probes, resulting in the formation of many biotin-labeled DNA duplexes, considerably amplifying the protein recognition event and facilitating the subsequent strengthening of the enzymatic signal, resulting in the formation of an ultrasensitive electrochemical aptamer sensor. The proposed aptasensor detects 0.82 pg/mL with a linear range of 1 pg/mL to 1 ng/mL.

VEGF is a protein widely used in the detection of adapter sensors. Table 1 summarizes the application of electrochemical aptasensor for VEGF detection and their performance and those mentioned above.

Table 1. Summary of recent published VEGF electrochemical aptasensor with the performance.

Sensor	Linear range	LOD	Reference
MGCE/Fe ₃ O ₄ /Fe ₂ O ₃ @Au-DNA	0.26–260 fM	0.26 fM	[81]
Target-induced conformational change/ methylene blue-modified aptamer	50 pM–0.15 nM	5 pM	[82]
Self-assembly of thiolated aptamers on gold- covered surface	0.15–100 ng/mL	0.15 ng/mL	[83]
Capacitive aptamer–antibody based sandwich assay	5 pg/mL – 1 ng/mL	401 pg/mL	[84]
Electrochemically triggered click reaction	0–10 μM	6.2 nM	[85]
BSA-gold nanoclusters/IL/GCE	1–120 pM	0.32 pM	[86]
rGO-PAMAM/AuNPs/thionine	2.5–320.0 pM	0.7 pM	[87]
Silicon nanowire	–	1.04 nM	[88]
PPy-NDFLG	–	100 fM	[89]

4. DETECTION OF PLATELET-DERIVED GROWTH FACTOR

Platelet-derived growth factor (PDGF) is a proangiogenic factor isolated from human platelets. PDGF receptor is a member of the tyrosine kinase family, which can promote cell chemochemization, division, and proliferation, and play a positive and important role in the body growth and development, wound repair, and other physiological processes [90–94]. As one of the angiogenic factors, PDGF is closely related to the occurrence and development of tumors. Tumor blood vessels are the pathological basis for tumor growth and metastasis [95]. On the one hand, tumors obtain nutrition and oxygen from the host through tumor blood vessels [96]. On the other hand, it also delivers metastatic cells to the host through tumor blood vessels and continues to grow and induce angiogenesis in other

parts of the body, leading to tumor metastasis. PDGF can also indirectly promote angiogenesis and tumor cell growth by inducing VEGF expression [97,98].

Wang et al. [99] described an electrochemical approach for determining PDGF that incorporates a sandwich structure and gold nanoparticle-mediated amplification. The findings demonstrate that this sensor with a "sandwich" structure and Au-NPs may considerably magnify the signal of PDGF detection using the electrochemical probe $[\text{Ru}(\text{NH}_3)_5\text{Cl}]^{2+}$, hence increasing sensing sensitivity dramatically. As a result, the detection limit of this PDGF test is very low: 1×10^{-14} M for purified samples and 1×10^{-12} M for contaminated samples or undiluted serum. Lai et al. [100] described direct sensing of PDGF in serum using an electrochemical, aptamer-based (E-AB) sensor. Using the E-AB technique, AC voltammetry is used to evaluate target-induced folding in methylene blue-modified PDGF-binding aptamers. The sensor is susceptible, highly selective, and almost reagent-free. This sensor can directly detect type BB PDGF in unadulterated, unaltered serum. This sensor's sensitivity and selectivity are equivalent to or much better than those of the best comparable optical techniques. For example, 50% serum can detect more than 25 million times the number of contaminated blood proteins, a fourfold increase over the most sensitive optical PDGF aptamer sensor known to date. Liu et al. [101] used a hydrothermal technique to build an electrochemically sensitive sensor for PDGF-BB detection based on leaf-like VS2 nanosheets. We created electrochemical aptamers by depositing gold nanoparticles on VS2-modified glassy carbon electrodes and then immobilizing them. The sensor has a detection limit of 0.4 pM for PDGF-BB. The detection range is linear and ranges from 0.001 nM to 1.0 nM. Degefa et al. [102] described a label-free PDGF aptasensor sensor. The aptamer sensor utilizes a hybrid self-assembled monolayer consisting of thiol-modified PDGF-binding aptamer and 6-mercaptohexanol. $[\text{Fe}(\text{CN})_6]^{3-/4-}$ was utilized as indicator ions to produce protein-aptamer complexes. The target protein may be detected effectively on the electrode surface using PDGF-binding aptamer SAMs without modifying the aptamer. Consistent with this finding, control studies utilizing unconjugated oligonucleotides synthesized on the electrode surface demonstrated that no aptamer-protein complex was generated. In the protein concentration range of 1 to 40 nM, the DPV signal on the aptamer-functionalized electrode demonstrated a linear reduction in the labeled ion peak current. Therefore, label-free detection of PDGF protein on aptamer-modified electrodes has been established. Li et al. [103] described the development of a new core-shell nanostructure built of Cu-based MOFs and TpBD-COFs to detect PDGF-BB. The core Cu-MOFs serve as signaling tags without additional redox mediators, while the porous TpBDs serve as shells for immobilizing PDGF-BB-targeted bulk through solid interactions such as π -stacking, electrostatics, and hydrogen bonding of aptamers. Hybridization of MOFs and COFs and immobilization with analyte-specific aptamers offer a promising and generic strategy for creating an aptamer sensor.

PDGF is also a protein widely used in the detection of adapter sensors. Table 2 summarizes the application of electrochemical aptasensor for PDGF detection and their performance in addition to those mentioned above.

Table 2. Summary of recent published PDGF electrochemical aptasensor with the performance.

Sensor	Linear range	LOD	Reference
GOD/PBA/GNCs/GOD/P-Gra-GNPs/GCE	0.005–60 nM	1.7 nM	[104]
aptamer II/PDGF/aptamer I/3D-4MgCO ₃ ·Mg(OH) ₂ ·4H ₂ O-Au NPs/CHIT/GCE	0.1 pg/mL–10 ng/mL	0.03 pg/mL	[105]
Protein-templated cobaltous phosphate nanocomposites	0.01–100 ng/mL	3.7 pg/mL	[106]
Aptamer and HAP nanoparticles	0.1 pg/mL–10 ng/mL	0.05 pg/mL	[107]
GCE β-CD/g-C ₃ N ₄ /CS Ad-DNA BSA Fc-DNA PDGF-BB	2×10^{-14} – 2×10^{-8} M	1.04×10^{-14} M	[108]
HT/Apt I/AuNPs/O-GS/GCE	0.002–40 nM	0.6 pM	[109]
GCE/thiolated hairpin-aptamer/MCH/PDGF-BB/biotinylated primer/dNTPs/Klenow Fragment polymerase.	0.1 ng/mL–120 ng/mL	1.8 pM	[110]
Au/EcoRI endonuclease	20 pg/mL–200 ng/mL	10 pg/mL	[111]

5. CONCLUSION

Detection of cancer-associated growth factors is very important for cancer typing, diagnosis and treatment. Based on the growth factor markers in tumor serum, this review summarized and compared the commonly used electrochemical aptamer detection methods. However, in the face of the presence of trace biomarkers in clinical samples, improving the sensitivity, specificity and practicability of electrochemical biosensing methods is still an important task at present. Throughout the current research, electrochemical biosensing methods of cancer-related growth factors have the following development trends.

(1) Enrich the variety of single-target detection. There are only a few biomarkers detected in the study, so more biomarkers can be developed to broaden the ideas and means of electrochemical detection of serum tumor biomarkers.

(2) Increase the number of multi-target detection. Serum tumor biomarker analysis remains focused on single and double biomarker detection. Selecting multiple typical markers of specific tumors for combined detection can make the detection more specific and improve tumor detection's sensitivity and sensing rate.

(3) Improve the practicality of sensor detection. Electrochemical biosensors are not effective in detecting biomarker molecules in human samples. Future research will focus on effectively combining sensor design with population sample pre-processing, integrating target extraction, enrichment, and sense, and effectively improving the practicality of the sensor.

References

1. D. Sadighbayan, K. Sadighbayan, M.R. Tohid-Kia, A.Y. Khosroushahi, M. Hasanzadeh, *TrAC Trends Anal. Chem.*, 118 (2019) 73.

2. A. Khanmohammadi, A. Aghaie, E. Vahedi, A. Qazvini, M. Ghanei, A. Afkhami, A. Hajian, H. Bagheri, *Talanta*, 206 (2020) 120251.
3. K.M. Koo, N. Soda, M.J. Shiddiky, *Curr. Opin. Electrochem.*, 25 (2021) 100645.
4. F. Cui, Z. Zhou, H.S. Zhou, *J. Electrochem. Soc.*, 167 (2019) 037525.
5. P. Fu, S. Xing, M. Xu, Y. Zhao, C. Zhao, *Sens. Actuators B Chem.*, 305 (2020) 127545.
6. S. Singh, A.A. Gill, M. Nlooto, R. Karpoomath, *Biosens. Bioelectron.*, 137 (2019) 213.
7. D. Sadighbayan, K. Sadighbayan, A.Y. Khosroushahi, M. Hasanzadeh, *TrAC Trends Anal. Chem.*, 119 (2019) 115609.
8. Y. Yang, Y. Fu, H. Su, L. Mao, M. Chen, *Biosens. Bioelectron.*, 122 (2018) 175.
9. M. Sadeghi, S. Kashanian, S.M. Naghib, F. Haghirsadat, D. Tofighi, *Int J Electrochem Sci*, 17 (2022) 2.
10. Y. Nur, S. Gaffar, Y.W. Hartati, T. Subroto, *Sens. Bio-Sens. Res.*, 32 (2021) 100416.
11. M. Negahdary, *Biosens. Bioelectron.*, 152 (2020) 112018.
12. M. El Aamri, G. Yammouri, H. Mohammadi, A. Amine, H. Korri-Youssoufi, *Biosensors*, 10 (2020) 186.
13. J. Quinchia, D. Echeverri, A.F. Cruz-Pacheco, M.E. Maldonado, J. Orozco, *Micromachines*, 11 (2020) 411.
14. R. Geetha Bai, K. Muthoosamy, R. Tuvikene, H. Nay Ming, S. Manickam, *Nanomaterials*, 11 (2021) 1272.
15. M. Hasan, M. Ahommed, M. Daizy, M. Bacchu, M. Ali, M. Al-Mamun, M.A.S. Aly, M. Khan, S. Hossain, *Biosens. Bioelectron. X*, 8 (2021) 100075.
16. D. Ou, D. Sun, Z. Liang, B. Chen, X. Lin, Z. Chen, *Sens. Actuators B Chem.*, 285 (2019) 398.
17. Y. Nur, S. Gaffar, Y.W. Hartati, T. Subroto, *Sens. Bio-Sens. Res.*, 32 (2021) 100416.
18. M. Hasanzadeh, N. Razmi, A. Mokhtarzadeh, N. Shadjou, S. Mahboob, *Int. J. Biol. Macromol.*, 108 (2018) 69.
19. L. Fu, S. Mao, F. Chen, S. Zhao, W. Su, G. Lai, A. Yu, C.-T. Lin, *Chemosphere*, 297 (2022) 134127.
20. Y. Zheng, D. Wang, X. Li, Z. Wang, Q. Zhou, L. Fu, Y. Yin, D. Creech, *Biosensors*, 11 (2021) 403.
21. D. Wang, D. Li, L. Fu, Y. Zheng, Y. Gu, F. Chen, S. Zhao, *Sensors*, 21 (2021) 8216.
22. Z. Shekari, H.R. Zare, A. Falahati, *Sens. Actuators B Chem.*, 332 (2021) 129515.
23. A. Nabok, H. Abu-Ali, S. Takita, D.P. Smith, *Chemosensors*, 9 (2021) 59.
24. E.M. Hassan, M.C. DeRosa, *TrAC Trends Anal. Chem.*, 124 (2020) 115806.
25. H. Karimi-Maleh, Y. Orooji, F. Karimi, M. Alizadeh, M. Baghayeri, J. Rouhi, S. Tajik, H. Beitollahi, S. Agarwal, V.K. Gupta, *Biosens. Bioelectron.* (2021) 113252.
26. H. Karimi-Maleh, A. Khataee, F. Karimi, M. Baghayeri, L. Fu, J. Rouhi, C. Karaman, O. Karaman, R. Boukherroub, *Chemosphere* (2021) 132928.
27. H. Karimi-Maleh, M. Alizadeh, Y. Orooji, F. Karimi, M. Baghayeri, J. Rouhi, S. Tajik, H. Beitollahi, S. Agarwal, V.K. Gupta, S. Rajendran, S. Rostamnia, L. Fu, F. Saberi-Movahed, S. Malekmohammadi, *Ind. Eng. Chem. Res.*, 60 (2021) 816.
28. H. Karimi-Maleh, F. Karimi, L. Fu, A.L. Sanati, M. Alizadeh, C. Karaman, Y. Orooji, *J. Hazard. Mater.*, 423 (2022) 127058.
29. H. Karimi-Maleh, C. Karaman, O. Karaman, F. Karimi, Y. Vasseghian, L. Fu, M. Baghayeri, J. Rouhi, P. Senthil Kumar, P.-L. Show, S. Rajendran, A.L. Sanati, A. Mirabi, *J. Nanostructure Chem.* (2022) in-press.
30. H. Karimi-Maleh, A. Ayati, S. Ghanbari, Y. Orooji, B. Tanhaei, F. Karimi, M. Alizadeh, J. Rouhi, L. Fu, M. Sillanpää, *J. Mol. Liq.*, 329 (2021) 115062.
31. H. Karimi-Maleh, A. Ayati, R. Davoodi, B. Tanhaei, F. Karimi, S. Malekmohammadi, Y. Orooji, L. Fu, M. Sillanpää, *J. Clean. Prod.*, 291 (2021) 125880.
32. H. Shi, L. Fu, F. Chen, S. Zhao, G. Lai, *Environ. Res.*, 209 (2022) 112747.

33. M. Chen, H. Yang, Z. Song, Y. Gu, Y. Zheng, J. Zhu, A. Wang, L. Fu, *Phyton-Int. Exp. Bot.*, 90 (2021) 1507.
34. Y. Xu, Y. Lu, P. Zhang, Y. Wang, Y. Zheng, L. Fu, H. Zhang, C.-T. Lin, A. Yu, *Bioelectrochemistry*, 133 (2020) 107455.
35. L. Fu, Y. Zheng, A. Wang, P. Zhang, S. Ding, W. Wu, Q. Zhou, F. Chen, S. Zhao, *J. Herb. Med.*, 30 (2021) 100512.
36. F. Shafiei, R.S. Saberi, M.A. Mehrgardi, *Bioelectrochemistry*, 140 (2021) 107807.
37. A. Norouzi, H. Ravan, A. Mohammadi, E. Hosseinzadeh, M. Norouzi, T. Fozooni, *Anal. Chim. Acta*, 1017 (2018) 26.
38. A. Raouafi, A. Sánchez, N. Raouafi, R. Villalonga, *Sens. Actuators B Chem.*, 297 (2019) 126762.
39. D. Sun, J. Lu, D. Chen, Y. Jiang, Z. Wang, W. Qin, Y. Yu, Z. Chen, Y. Zhang, *Sens. Actuators B Chem.*, 268 (2018) 359.
40. S. Vandghanoooni, Z. Sanaat, R. Farahzadi, M. Eskandani, H. Omidian, Y. Omid, *Microchem. J.*, 170 (2021) 106640.
41. V. Ranganathan, S. Srinivasan, A. Singh, M.C. DeRosa, *Anal. Biochem.*, 588 (2020) 113471.
42. M. Chen, Y. Xu, J. Zhao, W. Zhong, L. Zhang, Y. Bi, M. Wang, *EBioMedicine*, 42 (2019) 304.
43. B. Yang, Q.G. Wang, M. Lu, Y. Ge, Y.J. Zheng, H. Zhu, G. Lu, *Front. Oncol.*, 9 (2019) 589.
44. A. Russo, T. Franchina, G. Ricciardi, A. Battaglia, M. Picciotto, V. Adamo, *Int. J. Mol. Sci.*, 20 (2019) 1431.
45. P.-C. Hsu, D.M. Jablons, C.-T. Yang, L. You, *Int. J. Mol. Sci.*, 20 (2019) 3821.
46. V. Gristina, U. Malapelle, A. Galvano, P. Pisapia, F. Pepe, C. Rolfo, S. Tortorici, V. Bazan, G. Troncone, A. Russo, *Cancer Treat. Rev.*, 85 (2020) 101994.
47. M.Á. López-García, I. Carretero-Barrio, B. Pérez-Mías, M. Chiva, C. Castilla, B. Vieites, J. Palacios, *Cancers*, 12 (2020) 1578.
48. C. Guo, Z. Li, F. Duan, Z. Zhang, F. Marchetti, M. Du, *J. Mater. Chem. B*, 8 (2020) 9951–9960.
49. G. Bezerra, C. Córdula, D. Campos, G. Nascimento, N. Oliveira, M.A. Seabra, V. Visani, S. Lucas, I. Lopes, J. Santos, F. Xavier, M.A. Borba, D. Martins, J. Lima-Filho, *Anal. Bioanal. Chem.*, 411 (2019) 6667.
50. X. Yan, Y. Song, J. Liu, N. Zhou, C. Zhang, L. He, Z. Zhang, Z. Liu, *Biosens. Bioelectron.*, 126 (2019) 734.
51. Y. Wang, S. Sun, J. Luo, Y. Xiong, T. Ming, J. Liu, Y. Ma, S. Yan, Y. Yang, Z. Yang, J. Reboud, H. Yin, J.M. Cooper, X. Cai, *Microsyst. Nanoeng.*, 6 (2020) 32.
52. M. Pourmadadi, J.S. Shayeh, S. Arjmand, M. Omid, F. Fatemi, *Microchem. J.*, 159 (2020) 105476.
53. A. Zhang, G. Wang, L. Jia, T. Su, L. Zhang, *Int. J. Mol. Med.*, 43 (2019) 358.
54. R.B. de Aguiar, J.Z. de Moraes, *Front. Immunol.*, 10 (2019) 1023.
55. M. Xu, V.K. Yadavalli, *ACS Sens.*, 4 (2019) 1040.
56. R. Duan, X. Fang, D. Wang, *Front. Chem.*, 9 (2021) 361.
57. J. Liu, T. Yang, J. Xu, Y. Sun, *Front. Chem.*, 9 (2021) 488.
58. J. Zhou, Y. Zheng, J. Zhang, H. Karimi-Maleh, Y. Xu, Q. Zhou, L. Fu, W. Wu, *Anal. Lett.*, 53 (2020) 2517.
59. M. Kim, R. Iezzi Jr, B.S. Shim, D.C. Martin, *Front. Chem.*, 7 (2019) 234.
60. W. Kong, M.-H. Xiang, L. Xia, M. Zhang, R.-M. Kong, F. Qu, *Biosens. Bioelectron.*, 167 (2020) 112481.
61. M.-C. Hsu, M.-R. Pan, W.-C. Hung, *Cells*, 8 (2019) 270.
62. J. Li, S. Zhang, L. Zhang, Y. Zhang, H. Zhang, C. Zhang, X. Xuan, M. Wang, J. Zhang, Y. Yuan, *Front. Chem.*, 9 (2021) 339.
63. Z. Zhang, M. Peng, D. Li, J. Yao, Y. Li, B. Wu, L. Wang, Z. Xu, *Front. Chem.*, 9 (2021) 702.

64. L. Fu, X. Zhang, S. Ding, F. Chen, Y. Lv, H. Zhang, S. Zhao, *Curr. Pharm. Anal.*, 18 (2022) 4.
65. Z. Wu, J. Liu, M. Liang, H. Zheng, C. Zhu, Y. Wang, *Front. Chem.*, 9 (2021) 208.
66. Y. Yue, L. Su, M. Hao, W. Li, L. Zeng, S. Yan, *Front. Chem.*, 9 (2021) 479.
67. Z. Xu, M. Peng, Z. Zhang, H. Zeng, R. Shi, X. Ma, L. Wang, B. Liao, *Front. Chem.*, 9 (2021) 683.
68. C. Li, F. Sun, *Front. Chem.*, 9 (2021) 409.
69. S. Zhao, W. Yang, R.Y. Lai, *Biosens. Bioelectron.*, 26 (2011) 2442.
70. A. Ravalli, L. Rivas, A. De La Escosura-Muñiz, J. Pons, A. Merkoçi, G. Marrazza, *J. Nanosci. Nanotechnol.*, 15 (2015) 3411.
71. S. Ni, Z. Shen, P. Zhang, G. Liu, *Anal. Chim. Acta*, 1121 (2020) 74.
72. S. Ni, L. Qiao, Z. Shen, Y. Gao, G. Liu, *Electrochimica Acta*, 331 (2020) 135321.
73. Z. Lv, K. Wang, X. Zhang, *J. Immunoassay Immunochem.*, 35 (2014) 233.
74. X.-M. Fu, Z.-J. Liu, S.-X. Cai, Y.-P. Zhao, D.-Z. Wu, C.-Y. Li, J.-H. Chen, *Chin. Chem. Lett.*, 27 (2016) 920.
75. Y. Nonaka, K. Abe, K. Ikebukuro, *Electrochemistry*, 80 (2012) 363.
76. H. Wang, Y. Ma, C. Guo, Y. Yang, Z. Peng, Z. Liu, Z. Zhang, *Appl. Surf. Sci.*, 481 (2019) 505.
77. M. Amouzadeh Tabrizi, M. Shamsipur, L. Farzin, *Biosens. Bioelectron.*, 74 (2015) 764.
78. Y. Park, M.-S. Hong, W.-H. Lee, J.-G. Kim, K. Kim, *Biosensors*, 11 (2021) 114.
79. Z. Gao, F. Ren, G. Yang, G. Feng, L. Wu, G. Huang, Q. Chen, *Anal. Methods*, 13 (2021) 4934.
80. W. Cheng, S. Ding, Q. Li, T. Yu, Y. Yin, H. Ju, G. Ren, *Biosens. Bioelectron.*, 36 (2012) 12.
81. Y. Zhang, M. Liu, S. Pan, L. Yu, S. Zhang, R. Liu, *Appl. Surf. Sci.*, 580 (2022) 152362.
82. S. Zhao, W. Ma, L. Xu, X. Wu, H. Kuang, L. Wang, C. Xu, *Biosens. Bioelectron.*, 68 (2015) 593.
83. B.P. Crulhas, A.E. Karpik, F.K. Delella, G.R. Castro, V.A. Pedrosa, *Anal. Bioanal. Chem.*, 409 (2017) 6771.
84. A. Qureshi, Y. Gurbuz, J.H. Niazi, *Sens. Actuators B Chem.*, 209 (2015) 645.
85. L. Feng, Z. Lyu, A. Offenhäusser, D. Mayer, *Eng. Life Sci.*, 16 (2016) 550.
86. M. Shamsipur, L. Farzin, M.A. Tabrizi, F. Molaabasi, *Biosens. Bioelectron.*, 74 (2015) 369.
87. M.A. Tabrizi, M. Shamsipur, R. Saber, S. Sarkar, *Sens. Actuators B Chem.*, 240 (2017) 1174.
88. H.-S. Lee, K.S. Kim, C.-J. Kim, S.K. Hahn, M.-H. Jo, *Biosens. Bioelectron.*, 24 (2009) 1801.
89. O.S. Kwon, S.J. Park, J. Jang, *Biomaterials*, 31 (2010) 4740.
90. W. Li, W. Luo, M. Li, L. Chen, L. Chen, H. Guan, M. Yu, *Front. Chem.*, 9 (2021) 610.
91. S. Wei, X. Chen, X. Zhang, L. Chen, *Front. Chem.*, 9 (2021) 697.
92. Y. Chen, J. Gao, K. Yan, X. Yao, Y. Liu, J. Zhang, *Sens. Actuators B Chem.*, 316 (2020) 128130.
93. X. Lu, X. Wen, Z. Fan, *J. Lumin.*, 221 (2020) 117042.
94. X. Liu, F. Yang, D. Li, R. Yuan, Y. Xiang, *Sens. Actuators B Chem.*, 305 (2020) 127405.
95. X. Miao, Z. Zhu, H. Jia, C. Lu, X. Liu, D. Mao, G. Chen, *Sens. Actuators B Chem.*, 320 (2020) 128435.
96. D. Li, X. Li, B. Shen, P. Li, Y. Chen, S. Ding, W. Chen, *Anal. Chim. Acta*, 1092 (2019) 102.
97. Y. Saito, A. Yamaguchi, S. Nakamura, H. Okuyoshi, M. Shimazawa, H. Hara, *Neurosci. Lett.*, 727 (2020) 134930.
98. H. Zhao, Q. Liu, J. Wang, A. Huang, B. Qiu, Z. Lin, *Electrochimica Acta*, 399 (2021) 139423.
99. J. Wang, W. Meng, X. Zheng, S. Liu, G. Li, *Biosens. Bioelectron.*, 24 (2009) 1598.
100. R.Y. Lai, K.W. Plaxco, A.J. Heeger, *Anal. Chem.*, 79 (2007) 229.
101. X. Liu, H.-L. Shuai, K.-J. Huang, *Anal. Methods*, 7 (2015) 8277.
102. T.H. Degefa, J. Kwak, *Anal. Chim. Acta*, 613 (2008) 163.
103. Y. Li, Z. Liu, W. Lu, M. Zhao, H. Xiao, T. Hu, J. Ma, Z. Zheng, J. Jia, H. Wu, *Analyst*, 146 (2021) 979.
104. K. Deng, Y. Xiang, L. Zhang, Q. Chen, W. Fu, *Anal. Chim. Acta*, 759 (2013) 61.

105. C.-L. Zhao, M. Hua, C.-Y. Yang, Y.-H. Yang, *Chin. Chem. Lett.*, 28 (2017) 1417.
106. L. He, S. Zhang, H. Ji, M. Wang, D. Peng, F. Yan, S. Fang, H. Zhang, C. Jia, Z. Zhang, *Biosens. Bioelectron.*, 79 (2016) 553.
107. W. Jiang, D. Tian, L. Zhang, Q. Guo, Y. Cui, M. Yang, *Microchim. Acta*, 184 (2017) 4375–4381.
108. J. Gao, H. Xiong, W. Zhang, Y. Wang, H. Wang, W. Wen, X. Zhang, S. Wang, *Carbon*, 130 (2018) 416.
109. J. Han, Y. Zhuo, Y. Chai, R. Yuan, Y. Xiang, Q. Zhu, N. Liao, *Biosens. Bioelectron.*, 46 (2013) 74.
110. T. Yu, J. Li, Q. Liu, W. Cheng, D. Zhang, H. Ju, S. Ding, *Int J Electrochem Sci*, 7 (2012) 8533.
111. S. Zhang, X. Hu, X. Yang, Q. Sun, X. Xu, X. Liu, G. Shen, J. Lu, G. Shen, R. Yu, *Biosens. Bioelectron.*, 66 (2015) 363.

© 2022 The Authors. Published by ESG (www.electrochemsci.org). This article is an open access article distributed under the terms and conditions of the Creative Commons Attribution license (<http://creativecommons.org/licenses/by/4.0/>).